Environmental Science
Water Research & Technology

ROYAL SOCIETY OF CHEMISTRY

PAPER

View Article Online
View Journal | View Issue





Cite this: *Environ. Sci.: Water Res. Technol.*, 2023, **9**, 2338

# Removal of nonylphenol ethoxylate from laundry wastewater using modified and functionalized activated carbon†

Mahdieh Khajvand,[a] Patrick Drogui,[a]* Loick Pichon,[b] My Ali El Khakani,[b] Rajeshwar Dayal Tyagi[cd] and Emmanuel Brien[e]

Nonylphenol ethoxylate surfactants find wide applications in various industries. These surfactants could be used mainly as washing agents, pesticides, and in textile and leather manufacturing. However, their presence in aquatic environments has raised significant global health concerns. To address this issue, we conducted a study to investigate the impact of surface chemical groups on the removal of nonylphenol ethoxylate (NPEO) from synthetic laundry wastewater using different samples of coal-based activated carbon. The following treatments were carried out to prepare a series of samples: acid treatment with 10% HCl at 75 °C, heat treatment at 900 °C under $N_2$ flow, and oxidation in 10% $HNO_3$ at 75 °C. The impact of carbon treatments on the $NPEO_{3-17}$ and COD adsorption were examined by conducting batch adsorption using the modified carbons and synthetic laundry wastewater (SLWW) containing NPEO with the ethoxylate chain in the range of 3 to 17. Unmodified and modified activated carbon samples were characterized in terms of structural, morphological and chemical properties. The samples obtained by thermal treatment under $N_2$ flow at 900 °C achieved the highest removal efficiency (of up to 99%) for the adsorption of $NPEO_{3-17}$. Our results have proven that the highly improved removal efficiency of $NPEO_{3-17}$ is due to the increase of surface hydrophobicity of the heat-treated activated carbon. When the concentrations were below the critical micelle concentration, the ethoxylated surfactants are adsorbed as monomers by their hydrophobic moiety on a hydrophobic surface of activated carbon. Additional experiments were carried out to describe the sorption phenomenon, followed by the determination of the kinetic of $NPEO_{3-17}$ and COD removal using modified activated carbon. The application of Langmuir isotherm provided the best fit for $NPEO_{3-17}$ removal and allowed the determination of the adsorption rate constant ($K_a$ = 0.0506 L $\mu g^{-1}$) and the maximum adsorption capacity ($Q_m$ = 2168.3 $\mu g\ g^{-1}$). The initial adsorption rate for COD removal was 420 mg $g^{-1}$ $min^{-1}$. After ten cycles, the COD removal efficiency reduced from 80% to 50%, indicating the presence of unoccupied active sites in the activated carbon.

Received 5th May 2023,
Accepted 2nd July 2023

DOI: 10.1039/d3ew00329a

rsc.li/es-water

## Water impact

Nonylphenol ethoxylates (NPEOs) are commonly used in various applications, such as washing agents, but they are known to be endocrine disruptors and can have harmful effects on the environment. When NPEOs are released into the environment, they can break down and produce nonylphenol (NP), which is extremely toxic to aquatic organisms, even in low concentrations. To address this issue, we propose a reliable method for modifying activated carbon to increase its capacity for removing $NPEO_{3-17}$ from laundry wastewater before discharge into the sewage network. This approach will help to mitigate the negative impact of NPEOs and NP on the environment and aquatic life.

[a] *Institut National de la Recherche Scientifique (INRS), Centre-Eau Terre Environnement (ETE), Université du Québec, 490 Rue de la Couronne, Québec, G1K 9A9, Canada. E-mail: patrick.drogui@inrs.ca; Fax: +1 418 654 2600; Tel: +1 418 654 3119*
[b] *Institut National de la Recherche Scientifique (INRS), Centre- Énergie, Matériaux et Télécommunications (EMT), 1650 Boulevard Lionel-Boulet, Varennes, Québec, J3X 1P7, Canada*
[c] *School of Technology, Huzhou University, Huzhou, Zhejiang, China*
[d] *BOSK Bioproducts, Québec, Québec, Canada*
[e] *Groupe Veos Inc, 1552 rue Nationale, Terrebonne, Québec, J6W 6M1, Canada*

† Electronic supplementary information (ESI) available. See DOI: https://doi.org/10.1039/d3ew00329a

# 1. Introduction

A variety of industrial applications make use of alkylphenol ethoxylate (APEO) surfactants, including pulp and paper production, textile production, paint and coatings, adhesives, leather products, rubber and plastic production, metalworking (as lubricants), and agriculture. Nevertheless, their primary use is in the production of detergents for both household and industrial purposes. This is mainly due to their remarkable characteristics, such as relative ionic insensitivity and high absorptive behaviour.[1] APEOs are comprised of a hydrophobic phenol ring with varied alkyl chains and a hydrophilic chain with 1–100 ethoxylated groups (EO). Around 80% of APEOs represent nonylphenol ethoxylates (NPEO), and the remaining is octylphenol ethoxylates (OPEO).[2]

The APEOs are unstable in the environment and, as a result of their use, discharge, and biodegradation, break down into less biodegradable products, including low-mole ethoxylates (mono- and diethoxylates), ether carboxylates, acidic derivatives, and alkylphenol under anoxic conditions.[3,4] Nonylphenol (NP) and octylphenol (OP) have become global environmental concerns due to long-distance transportation, persistence against biological degradation, and an inclination for bioaccumulation in fatty tissues. They are also extremely toxic to aquatic organisms, even at sorely low concentrations and are weakly estrogenic.[4–6]

Nonylphenol and its ethoxylates have been banned in the European Union by the Water Framework Directive 2003/53/EC (European Commission 2003). It is, however, technically and economically impossible to substitute them with alternative chemicals in some industrial applications.[7] In the USA, the Environmental Protection Agency (EPA) has issued a recommendation stating that the NP concentrations should not exceed 6.6 and 1.7 μg $L^{-1}$ in freshwater and saltwater, respectively. In addition, these emerging compounds exert endocrine disruption effects on marine organisms since they mimic natural hormones by interacting with estrogen receptors.[8] It is thus essential to eliminate the APEOs from laundry wastewater before discharging them to the sewage treatment plant, where microorganisms decompose the ethoxy chains to NP and OP. Conventional technologies are poorly efficient in eliminating these refractory and non-biodegradable substances.[7] Therefore, employing a developed technology such as advanced oxidation processes (AOPs) or hybrid processes can overcome this problem and reach treated water with reuse quality.[9]

One of the proposed technologies for the removal of APEOs is adsorption. Adsorption is a surface phenomenon used to remove both organic and inorganic pollutants.[8] In this process, a solid substance called an adsorbent is introduced into the wastewater that is contaminated with pollutants. The adsorbent selectively attracts and captures specific pollutants onto its surface. Once pollutants are captured, the adsorbent can undergo regeneration through the process of desorption. This process effectively removes the pollutants from the adsorbent, allowing it to be reused.[10] Several factors can influence the adsorption of a pollutant from wastewater, including i) the porosity and the chemical nature of the adsorbent, ii) the nature and structure of the constituents of the wastewater, iii) the concentration of the pollutant in wastewater, iv) salts and molecules in the aqueous phase that can compete for adsorption sites, v) the adsorption time, and vi) the pH of the solution.[2] Several studies were carried out to remove APEOs by adsorption into various adsorbents. Thomas *et al.* (1987) studied the adsorption of octylphenol ethoxylate (TX-100) onto silica, alumina, and activated carbon (AC) and discussed the enthalpy curve of these adsorbents.[11] The adsorption of APEOs from an aqueous solution using β-cyclodextrin polymer (βCD-P) was studied by Murai *et al.* (1996). They concluded that about 85% of APEOs were removed by βCD-P.[12] Nikolenko *et al.* (2002) investigated the adsorption of NPEOs from their micellar solutions on silica gel.[13] Other groups used synthetic resins for the adsorption of $NPEO_{10}$ and their subsequent removal from aqueous solutions.[14,15] Mostafazadeh *et al.* (2019) employed various integrated treatments, including ultrafiltration followed by adsorption using resin and activated carbon, to eliminate $NPEO_{3–17}$ from real laundry wastewater.[16] In another study, researchers explored the effectiveness of employing a submerged membrane filtration system in combination with powdered activated carbon to remove $NPEO_{1–15}$.[17] In a more recent study conducted by Čižmárová *et al.* (2022), the researchers explored the effectiveness of combining ozonation with adsorption using granular activated carbon, Fe-modified zeolite, and Mn-modified zeolite in order to remove alkylphenol ethoxylates from pre-treated industrial wastewater.[18]

A variety of substances have been developed for adsorbing non-ionic surfactants.[19–23] The application of adsorbents mainly depends on the porous medium's surface chemistry and pore structure. Activated carbon is one of the most suitable adsorbents for removing non-ionic surfactants. Therefore, researchers' main focus has been enhancing activated carbon's potential for removing these contaminants by introducing functional groups on their surface. Various methods, including acid, heat, impregnation, or microwave treatments, have been studied to develop surface-modified activated carbons.[24] Some investigations were performed for functionalizing carbons to remove APEO, mostly OPEO, from synthetic wastewater.[21,22,25] Soria-Sánchez *et al.* (2010) used graphite and a microporous activated carbon and modified it by heat and acid treatments to eliminate a series of non-ionic surfactants (TX-114, TX-100, TX-165, and TX-305). To introduce oxygen surface groups, adsorbents were treated with nitric acid. Both materials demonstrated different adsorption behavior when oxygen surface groups were introduced onto carbonaceous surfaces. For graphite, the adsorbed amounts below the critical micelle concentration (CMC) decreased, and above the CMC increased slightly. The probable reason for the reduction in the adsorption efficiency

below the CMC has been attributed to the withdrawal effect of the oxygen surface groups. On the contrary, by oxidizing AC with nitric acid, adsorbed uptakes below and above CMC showed an increase, which was explained by the interaction of surfactant molecules with oxygen surface groups inside the micropores.[25]

The chemical oxygen demand (COD) is a critical parameter that is assessed along with surfactant concentration in LWW. The COD concentration was used as a reference in removing organic contaminants. It was discovered that there is a strong relationship between COD and surfactant concentrations.[26,27] Therefore, in this study, we measured COD removal percentage as a preliminary analysis.

The primary objective of the present study is to develop a reliable method for the modification of activated carbon in order to enhance its capacity for removing $NPEO_{3-17}$ and COD from laundry wastewater. For this purpose, a sequence of treatments, including acid treatment, heat treatment, and oxidation with $HNO_3$, was carried out on activated carbon samples. The specific objectives consist in characterizing the adsorbents. The material characterizations of the treated AC samples provided elements for the interpretation of $NPEO_{3-17}$ and COD removal from laundry wastewater. Finally, in order to describe the sorption phenomenon, a series of experiments were conducted. Our results demonstrate the possibility of removing up to 99% of $NPEO_{3-17}$ in laundry wastewater by using the appropriate treatment of activated carbon.

## 2. Experimental procedure

### 2.1. Material

The treatment process was carried out in synthetic laundry wastewater (SLWW). The SLWW was prepared by dissolving a detergent, GE Boost from Gurtler Company, in distilled water. Nitric acid (70%), hydrochloric acid (34–37%), dichloromethane (99+%), and methanol (Peroxide-Free/Sequencing) were obtained from Fisher Scientific (Ottawa, ON, Canada). Formic acid was purchased from Honeywell. Supelclean™ ENVI-Carb™ SPE tube (500 MG/6 ML) was purchased from Sigma Aldrich (Oakville, ON, Canada). Surrogate was obtained from Cambridge Isotope Laboratories, Inc.

Three different coal-based ACs were employed to run experiments. Granular activated carbons (GAC) were supplied, including HYDRODARCO® 3000 (HD) from Cabot Norit Activated Carbon, FILTRASORB® 400 (F400) from Calgon Carbon Corporation, and ProLine® (P) from pentair Aquatic Eco-System Inc. The characteristics of the adsorbents are shown in Table 1. All activated carbons were grounded and sieved, and the particles with a size between 0.250 to 0.500 mm and 0.500 to 1.00 mm were collected. Several studies[28,29] suggested washing the GAC with ultrapure water and drying it at 105 ± 5 °C overnight. The reason for washing is to remove dust[30,31] and drying at 105 °C to remove any adsorbed moisture before use.[32] Then, it should be kept in a desiccator at room temperature (20 ± 2 °C) before experiments.

### 2.2. Functionalizing activated carbons

Functionalizing GAC aims to enhance the activated carbon capability to simultaneously remove $NPEO_{3-17}$ and COD from LWW. The GAC was prepared as described by Soria-Sánchez (2010) with modifications.[25] The modified carbons were labelled with abbreviation codes characterizing the pretreatment processes used since different treatment approaches were used. Each modified carbon was identified by its original precursor, followed by codes that described the pretreatment steps. A brief overview of carbon treatment pathways is provided in this section.

**2.2.1. Treatment with hydrochloric acid.** Before surface treatments, the inorganic contaminants on the AC were removed with HCl. 1 gr of GAC was mixed with 10 mL of 10% HCl and heated at 75 °C until almost all HCl acid was evaporated. This procedure was repeated twice. The sample was washed with distilled water at room temperature (20 ± 2 °C) until the total elimination of free chloride ions (pH = 6). Afterward, the sample was dried in a vacuum oven at 110 °C overnight. The resulting carbon was denoted as $AC_{Cl}$.

**2.2.2. Heat treatment under nitrogen gas.** A tubular quartz reactor horizontally positioned within a tubular furnace was filled with a 5 g sample. The samples were subjected to a one-hour treatment at 900 °C under nitrogen flow. The heat-

Table 1 Characteristics of activated carbons

| Name | ProLine® | HYDRODARCO® 3000 | FILTRASORB® 400 |
|---|---|---|---|
| Characteristics | | | |
| Abbreviation | P | HD | F400 |
| Carbon type | Activated bituminous coal | High-temperature steam activation of lignite coal | Bituminous coal |
| Hardness | >90% | | |
| Iodine number (mg $gm^{-1}$) | >928 | >500 | >1000 |
| Ash content | <6% | | |
| Dust | | <0.3% | |
| Moisture as packet | <5% | <8% | <2% |
| Apparent density (g $mL^{-1}$) | >0.41 | 0.38 | 0.54 |
| Surface area (min) ($m^2$ $g^{-1}$) | 1050 | | |

 

treated samples were marked with the HT codes ($AC_{HT}$). This procedure leads to the elimination of surface groups, especially oxygenated ones.

**2.2.3. Treatment with nitric acid.** The sample was mixed with $HNO_3$ (10% wt concentration) to introduce oxygen surface groups. The mixture was stirred and heated at 75 °C until almost all the liquid evaporated. The ratio AC/$HNO_3$ was 1 g to 10 mL. The procedure was repeated three times. The resulting sample was washed with distilled water at room temperature (20 ± 2 °C) until pH = 6. Afterward, the sample was dried in a vacuum oven at 110 °C overnight and kept in a desiccator for further experiments. The nitric acid-oxidizing sample was referred to $AC_{HN}$.

A total of 15 activated carbons were obtained by combining these techniques. The name of a sample reflects the sequence of various treatment steps employed. $F400_{Cl,HT,HN}$, for instance, is the name for F400 carbon that was subjected to the processes outlined in this section, which included hydrochloric acid treatment, heat treatment under nitrogen at 900 °C for one hour, and nitric acid oxidation.

### 2.3. Adsorption procedure

Adsorption experiments were carried out in Erlenmeyer shake flasks containing the same amount of the modified and unmodified GACs used as a sorbent (150 mg of GAC was added to 60 mL of SLWW). The SLWW was prepared by mixing 270 μL detergent (GE Boost) in 1 L distilled water. Three different types of experiments were successively run. The first part consisted in conducting effectiveness tests to determine the adsorption capacity of $NPEO_{3-17}$ in SLWW. The flasks were shaken at 150 rpm at room temperature 20 ± 2 °C, pH = 7.0 ± 0.5 for 3 h. Then the solution were filtrated through a 0.22 μm MF-Millipore™ membrane filter, and the residual $NPEO_{3-17}$ and COD concentrations were measured. Subsequently, isotherm adsorption experiments were carried out using different amounts of adsorbents (600, 457, 186, 150, 62, and 22 mg) added in 60 mL SLWW and was shaken up to 3 h with 150 rpm. Temperature and pH were initially maintained at 20 ± 2 °C and 7.0 ± 0.5, respectively. The maximal adsorption capacity and the relationship between the adsorbent and adsorbate are both shown by the adsorption isotherm. A set of equilibrium concentration data between the amount of adsorbate in the adsorbent ($q_e$) and the amount of adsorbate still present in the liquid phase ($C_e$) were gathered under equilibrium circumstances in order to derive an adsorption isotherm. The relation between $C_e$ and $q_e$ according to the mass balance is given by eqn (1):[33]

$$q_e = \frac{(C_0 - C_e)V}{m} \quad (1)$$

$V$ and $m$ are the initial volume of the solution and the mass of the adsorbent.

The rate of the adsorbent to the volume of the solution can be adjusted between 0.25 and 10 (mg $mL^{-1}$).[30,34,35] The maximal adsorption capacity and the interactions between the adsorbent and adsorbate are described by the equilibrium isotherms. The isotherm models and experimental data would be evaluated, and the best match would be determined. Different adsorption isotherm models were used for curve-fitting, including Langmuir,[36] Temkin,[37] Freundlich,[38] Redlich–Peterson,[39] and Liu.[40]

Giles *et al.* (1960) classified adsorption isotherms into four major types based on the initial slope of the curves. The four basic categories are (i) S curves, known as vertical orientation types, (ii) L curves, known as normal or "Langmuir" types, (iii) H curves, known as high-affinity types; and (iv) C curves, known as constant partition types. The subgroups are identified by the shape of the upper parts of the curves, including plateau and changes in slope, and denoted by 1, 2, 3, 4, and mx.[41] This classification has been used to diagnose the adsorption mechanism of $NPEO_{3-17}$ and COD in the modified activated carbon.

If the concentration of the specific adsorbate in the solution declines from $C_0$ to $C_e$ at the end of the operation, the removal efficiency ($R$) would be calculated by eqn (2):

$$R = \frac{C_0 - C_e}{C_0} \times 100 \quad (2)$$

According to the second set of assays, adsorption kinetic was evaluated using 200 mL of SLWW in the presence of 500 mg of sorbent. The flasks were shaken at 150 rpm at room temperature (20 ± 2 °C), and samples were taken at interval times (0.3, 1.3, 3.0, 8.0, 19.5, 24.5, 30.0, 48.0 h). Samples were collected using 0.22 μm Millex syringe filters, and residual COD concentrations were measured. Investigation of the $NPEO_{3-17}$ adsorption kinetics was not feasible for this work, since each analysis requires a minimum of 50 mL of the solution to quantify $NPEO_{3-17}$. Given the initial volume of the solution (200 mL), it was not possible to maintain equilibrium conditions while taking samples at the specified intervals. As a result, COD was measured at time intervals, and COD was used as a reference in absorption kinetics. Several models are reported in the literature, but in this study, five kinetic models were used. The pseudo-first-order model,[42] the pseudo-second-order model,[43] Elovich model,[44] second-order rate model,[45] and intraparticle diffusion[46] were respectively used.

The third set of assays consisted in evaluating the changes in the removal efficiency in case of consecutive adsorption cycles. Regeneration of the exhausted adsorbent is essential for its practical usage. In this regard, the batch adsorption process with 150 mg of adsorbent was conducted for ten consecutive cycles. After each cycle, the adsorbent was dried at 105 ± 5 °C for 2 h and reused under the same experimental conditions with 60 mL of fresh SLWW. This experiment aimed to find a suitable number of cycles for repeated use of the adsorbent without a considerable decrease in their adsorption capacity. After ten adsorption cycles, regeneration by thermal treatment at 900 °C under nitrogen for 90 min was performed using activated carbon.

### 2.4. Instruments and analysis

A tubular furnace (Lindberg/Blue M™ Mini-Mite™ Tube Furnaces) and a quartz tube horizontally positioned inside was used to apply heat treatment on activated carbon.

To do the adsorption process, an orbit shaker (Lab-Line Orbit Shaker Model 3520) was used.

The structure and morphology of the as-received and functionalized GAC were determined by Fourier transform infrared (FTIR) and scanning electron microscopy (SEM). Fourier transform infrared attenuated total reflectance (FTIR-ATR) spectra were recorded on a Nicolet iS50 spectrometer (Thermofisher Scientific, USA) at 0.04 $cm^{-1}$ resolution and in the range of 400–4000 $cm^{-1}$. The surface morphology of the samples was examined by means of SEM observations (Carl Zeiss EVO® 50 smart SEM, USA) at an operating voltage of 15 kV. The samples were gold-coated. The elemental analysis of the particles present on the surface is enabled by an energy dispersive X-ray spectrometry (EDS) Microanalysis System (model: Bruker Quantax 800/Z30 SSD, Germany). This EDS is equipped with an Xflash® 6|30 Silicon drift detector (SDD). It can detect elements from Beryllium ($z$ = 4) to Uranium ($z$ = 92).

The specific surface area, average pore size and volume were carried out *via* the gas adsorption technique. The $N_2$ adsorption isotherms at a liquid nitrogen temperature of −196 °C (77 K) were measured on a Micromeritics ASAP 2020 surface area analyzer. Before the analysis, the AC samples were thoroughly rinsed (to remove heavy volatile organic compounds) and dried at 110 °C. Then they were further *in situ* outgassed at 110 °C. The Brunauer–Emmett–Teller (BET) approach was used in the adsorption mode to derive the BET surface area of the samples, while the Barrett–Joyner–Halenda (BJH) analysis was used to evaluate the pore size of the activated carbon samples in both adsorption and desorption regimes. A typical complete adsorption/desorption BJH experiment requires almost 10 h per sample.

A UV-type spectrophotometer 0811 M136 (Varian brand, Canada Inc.) was used to measure UV/vis spectra. The UV/vis spectra were carried out as described by Mokhtarifar (2018) with minor modifications.[47] We prepared the UV samples by dispersing 0.05 g of each finely powdered sample in 200 mL of distilled water and sonicating the suspension for 1 h. A further 24 h rest was given to the resulting samples to ensure they were stable. Finally, 3.5 ml of the final solution was converted into quartz cuvettes to measure the transmittance of the solution in the wavelength range of 200 to 800 nm.

COD was analyzed by a UV-type spectrophotometer 0811 M136 (Varian brand, Canada Inc) according to the analytical method (MA 315-DCO 1.1) of the center of expertise in environmental analysis. For the high-level COD measurements ranging from 80 to 800 mg $L^{-1}$ $O_2$, a calibration curve was established using standard solutions of 0, 100, 300, 500, 800, and 1000 mg $L^{-1}$. The absorbance of these solutions was measured at 600 nm. However, for the low-level COD measurements spanning from 5 to 100 mg $L^{-1}$ $O_2$, a calibration curve was created using standard solutions of 0, 10, 30, 70, 500, and 100 mg $L^{-1}$. The absorbance of these solutions was measured at 420 nm.

The method of MA 400 – NPEO 1.1 was used to evaluate the concentration of $NPEO_{3-17}$. Sample preparation included four phases: washing, conditioning, extraction, and recovery. In the washing phase, the carbon cartridge (tube) was washed in three steps, twice with 6 mL of dichloromethane, twice with 6 mL of a standard solution (containing methanol, dichloromethane, and formic acid), and finally twice with 6 mL of dichloromethane. The conditioning phase included two steps of adding 6 mL of methanol followed by 20 mL of 2 N hydrochloric acid to the tube. In the extraction phase, the acidified sample with hydrochloric acid (to pH = 3) added 100 μl of surrogate 1 ppm was passed through the tube. The $NPEO_{3-17}$ were subsequently extracted because of their passage through the carbon cartridges. In the last phase, the recovery phase, 9 mL of the standard solution was passed through the tube, and the solution containing $NPEO_{3-17}$ was collected. The collected solution was subjected to nitrogen gas until the completely extracted solution was dried. Then, the residue was dissolved in 1 mL of methanol. The sample was finally passed through liquid chromatography coupled with a tandem mass spectrometer (LC-MS/MS).[16]

## 3. Results and discussion

### 3.1. NPEO and COD removal

One of the most favorable materials for applying liquid phase treatment, including organic matter, is AC. The removal efficiency of the functionalized activated carbon samples was compared to non-functionalized-AC ones in batch experiments. Different adsorbent materials (P, HD and F400) described in Table 1 were used. The residual COD concentrations and the percentage of COD removal as a function of adsorbent materials were reported in Table 2. The removal percentage of AC was reported in two particle size ranges, 0.250–0.500 and 0.500–1.00 mm. The average COD concentration in SLWW was 572.9 ± 55.0 mg $L^{-1}$.

According to the COD value obtained from the supernatant, the removal percentage increased by decreasing the particle size of activated carbon samples. Adsorption kinetics are accelerated due to the small particle size. Smaller particles have a shorter diffusion path, allowing easier access to the interiors of carbon particles. Additionally, increasing the number of particles is a benefit of decreasing particle size. The number of particles produced grows to the third power as the GAC diameter decreases. On the other hand, the handling and regeneration of smaller particles are more difficult.[48]

The samples modified by heat treatment and the samples subjected to acid treatment with HCl followed by heat treatment successfully improved the removal efficiency compared to non-functionalized AC. The maximum increase in COD removal was obtained at 18% for $P_{Cl,HT}$ owing to the particle size of 0.250–0.500 mm and 17% for $P_{HT}$ in both the

 

**Table 2** COD removal using different adsorbent materials (P, HD and F400) with or without pretreatment (conditions: initial COD = 572.9 ± 55.0 mg $L^{-1}$, $T$ = 20 ± 2 °C, pH = 7.0 ± 0.5, shaker speed = 150 rpm, treatment time = 180 min)

| Adsorbent materials | Particle size (0.250–0.500 mm) | | Particle size (0.500–1.00 mm) | |
|---|---|---|---|---|
| | Residual COD conc. (mg $L^{-1}$) | COD removal (%) | Residual COD conc. (mg $L^{-1}$) | COD removal (%) |
| P | 133.1 | 76.85% | 204.8 | 64.33% |
| $P_{Cl,HT}$ | 27.6 | 95.19% | 149.7 | 73.75% |
| $P_{Cl,HT,HN}$ | 296.6 | 50.85% | 250.7 | 55.87% |
| $P_{HT}$ | 35.6 | 93.93% | 120.8 | 79.13% |
| $P_{HT,HN}$ | 168.7 | 70.15% | 226.4 | 59.92% |
| HD | 73.5 | 88.11% | 153.7 | 73.33% |
| $HD_{Cl,HT}$ | 59.8 | 90.34% | 118.8 | 78.57% |
| $HD_{Cl,HT,HN}$ | 317.7 | 48.63% | 282.0 | 49.80% |
| $HD_{HT}$ | 33.8 | 94.53% | 114.7 | 79.39% |
| $HD_{HT,HN}$ | 358.9 | 41.97% | 272.6 | 51.61% |
| F400 | 131.3 | 78.77% | 217.0 | 64.91% |
| $F400_{Cl,HT}$ | 42.6 | 93.10% | 202.8 | 67.21% |
| $F400_{Cl,HT,HN}$ | 301.1 | 51.31% | 334.7 | 45.88% |
| $F400_{HT}$ | 53.9 | 91.29% | 152.1 | 75.40% |
| $F400_{HT,HN}$ | 308.6 | 50.10% | 319.9 | 48.27% |

P = Proline® activated carbon; HD = Hydrodarco®-3000; F400 = Filtrasorb®-400.

particle size of 0.250–0.500 and 0.500–1.00 mm, respectively. Generally, more significant improvement by heat treatment was observed for activated carbon with a smaller particle size. This might be related to more accessible access to the inner side of the carbon particles for modification due to the shorter pathway.

Considering COD removal efficiency and price of different activated carbons, the adsorbents were narrowed down, and $NPEO_{3-17}$ amounts were measured for solutions obtained from adsorption by ProLine®, Hydrodarco® 3000, and their derivative functionalized activated carbons. In order to observe the effect of the particle size in $NPEO_{3-17}$ removal, we applied adsorption into two particle ranges of ProLine®. Table 3 shows the $NPEO_{3-17}$ removal of the mentioned adsorbents. The average amount of $NPEO_{3-17}$ in the initial SLWW solution was measured at 971.3 ± 93.5 μg $L^{-1}$. The value of $NPEO_{3-17}$ in real laundry wastewater was reported in a range of 260–2400 μg $L^{-1}$.[16] Therefore, the amount of $NPEO_{3-17}$ in the solution was within the reported range.

The percentage of $NPEO_{3-17}$ removal was reduced by increasing the particle size. However, the $NPEO_{3-17}$ removal efficiencies using respectively untreated and heat-treated activated carbons were still in the same range in spite of the particle size increase. The results indicated that the selected activated carbons could almost completely remove $NPEO_{3-17}$ in the synthetic solution under experimental conditions. Therefore, this amount of activated carbon (150 mg per 60 mL SLWW) provided enough available active sites to capture almost entirely $NPEO_{3-17}$ from the solution with an initial $NPEO_{3-17}$ concentration of 971.3 ± 93.5 μg $L^{-1}$.

Based on the study's findings, where untreated (P) and functionalized activated carbon ($P_{Cl,HT}$, and $P_{HT}$) achieved a remarkable removal rate of over 99% for $NPEO_{3-17}$, we decided to compare the efficiencies of two specific adsorbents, namely untreated activated carbon (P) and heat-treated activated carbon ($P_{HT}$). To ensure a fair evaluation, we subjected the adsorbents to a relatively low concentration of adsorbents (22 mg per 60 mL SLWW, equivalent to 0.37 g $L^{-1}$). Under these conditions, we observed that the use of P

**Table 3** $NPEO_{3-17}$ removal using different adsorbent materials (P and HD) with or without pretreatment (conditions: initial $NPEO_{3-17}$ = 971.3 ± 93.5 μg $L^{-1}$, $T$ = 20 ± 2 °C, pH = 7.0 ± 0.5, shaker speed = 150 rpm, treatment time = 180 min)

| Adsorbent materials | Particle size (0.250–0.500 mm) | | Particle size (0.500–1.00 mm) | |
|---|---|---|---|---|
| | Residual NPEO conc. (μg $L^{-1}$) | NPEO removal (%) | Residual NPEO conc. (μg $L^{-1}$) | NPEO removal (%) |
| P | 0.9 | 99.90% | 4.3 | 99.56% |
| $P_{Cl,HT}$ | 1.2 | 99.89% | 6.8 | 99.31% |
| $P_{Cl,HT,HN}$ | 2.2 | 99.78% | 53.8 | 94.46% |
| $P_{HT}$ | 0.5 | 99.95% | 4.3 | 99.54% |
| $P_{HT,HN}$ | 2.5 | 99.75% | 41.2 | 95.85% |
| HD | — | — | 4.6 | 99.51% |
| $HD_{Cl,HT}$ | — | — | 3.2 | 99.66% |
| $HD_{Cl,HT,HN}$ | — | — | 121.2 | 88.32% |
| $HD_{HT}$ | — | — | 3.3 | 99.66% |
| $HD_{HT,HN}$ | — | — | 89.4 | 90.92% |

P = Proline® activated carbon; HD = Hydrodarco®-3000.

resulted in a $NPEO_{3-17}$ removal efficiency of 41%. However, when the heat-treated sample, $P_{HT}$, was employed, the $NPEO_{3-17}$ removal efficiency improved significantly to 62%. Moreover, we measured the $NPEO_{3-17}$ adsorption capacities of 1550 μg $g^{-1}$ and 2092 μg $g^{-1}$ for P and $P_{HT}$, respectively. This comparison clearly demonstrates that the heat treatment of activated carbon plays a crucial role in enhancing the adsorption capacity for $NPEO_{3-17}$ removal, by an impressive 35%.

**3.1.1. Effect of specific surface area and the pore size.** Several factors affect the adsorption of NPEO from aqueous solutions, including the specific surface area and the pore size of the adsorbent.[14] It was found that the surface area of pores larger than 1.5 nm is crucial to the adsorption capacity of NPEO. Consequently, NPEO molecules might mainly adsorb on pores with a diameter greater than 1.5 nm.[49] In the following sections, we delved into a more comprehensive analysis and discussion of the characteristics of the adsorbent, focusing on specific surface area and pore size, and their impact on the removal of NPEO.

**3.1.2. Effect of acid treatment.** As a result of acid treatment, chemical reactions occur between the acid and the mineral matter. Depending on the treatment, pore structure, surface functionality, or adsorption capacity may change. In addition to introducing new functional groups, acid treatment can lead to the loss of some moieties. Varieties of acids react differently with the ash and the available functional groups. The most common method for removing ash is to use HCl.[50] On the other hand, treatment with $HNO_3$ forms acidic surface groups, especially carboxylic acids and, to a lesser extent, lactones, anhydrides, and phenols.[51] The introduction of functional groups can enhance surface acidity or generate charged sites on the carbon surface. Consequently, the altered surface charge has the potential to influence the electrostatic interactions between the adsorbent and NPEO, thereby influencing the adsorption capacity and selectivity. In other words, $HNO_3$ reduces the basic surface functional groups through oxidative effects.[52]

**3.1.3. Effect of heat treatment.** Heat treatment of activated carbon at high temperatures (>700 °C) under a flow of gases like nitrogen, helium, or hydrogen selectively removes some surface groups, especially oxygenated groups. It was reported that weakly acidic functionalities (such as carbonyl, phenol, and quinone) decompose at higher temperatures than strongly acidic functionalities (like carboxylic, anhydrides, and lactones).[53] By heat treatment, oxygen-acidic functional groups are thermally desorbed, resulting in the creation of unsaturated surfaces and an increase in the basicity of the carbon surface.[50] On the other hand, the resulting activated carbon possesses reactive sites capable of re-adsorbing oxygen, forming some of the previously removed groups. Thermal treatments under a flow of $H_2$ trigger to generate more stable basic surfaces compared to $N_2$ flow, thus preventing further adsorption of oxygen.[51]

Surfactants can be partially dissolved in water. They aggregate and form micelles if the concentration exceeds the CMC. For NPEO with 9–18 ethoxy units, the CMC value was reported to be 0.042 g $L^{-1}$ or 42 000 μg $L^{-1}$.[54] Therefore, the concentration of NPEO in a typical laundry wastewater (260–2400 μg $L^{-1}$),[16] and our initial solution (971.3 ± 93.5 μg $L^{-1}$) is lower than CMC. At concentrations below CMC, the ethoxylated surfactants are adsorbed as monomers by their hydrophobic moiety on a hydrophobic surface.[25] Therefore, the lower the oxygen groups on the surface of activated carbon and the higher the hydrophobicity of the surface, the higher the NPEO adsorption rate. Consequently, modification of the activated carbon by heat treatment at high temperature or initially acid treatment by HCl followed by heat treatment led to improving the removal efficiency of the NPEO by increasing the hydrophobicity of the activated carbon. It is worth noting that at concentrations above CMC, the surfactants form aggregates (micelles), and the adsorption mechanism differs from the above explanation.

By comparaison, Soria-Sánchez *et al.* (2010)[25] conducted a study examining the adsorption behavior of various octylphenol ethoxylate surfactants (TX-114, TX-100, TX-165, and TX-305) on modified graphite and wood-based activated carbon. The investigation focused on adsorption occurring below and above the critical micelle concentration (CMC). For the graphite material, the adsorbed quantities below the CMC were found to be higher on heat-treated graphite (GT) compared to the heat-treated sample followed by oxidation with $HNO_3$ (GTox). This difference was attributed to the withdrawal effect caused by the presence of oxygen surface groups. In contrast, above the CMC, the adsorbed quantities slightly increased on GTox compared to GT, suggesting improved micelle formation. On the other hand, the heat-treated activated carbon followed by $HNO_3$ oxidation (NTox) exhibited a remarkable increase in adsorbed uptakes both below and above the CMC when compared to the heat-treated sample (NT). This observation could be attributed to specific interactions between the surfactant molecules and oxygen surface groups within the micropores of the activated carbon.

It is critical in the batch study to determine the optimal adsorbent dose and contact time for maximum adsorbate removal. To achieve the first goal, an adsorption isotherm was carried out, and the adsorption kinetics was applied to obtain the latter purpose. To perform the adsorption isotherm, kinetics, and adsorption cycles; we chose $P_{HT}$ with a particle size of 0.500–1.00 mm. We considered three aspects to select the optimal adsorbent: type of adsorbent, modification, and particle size. Regarding the type of adsorbent, it was decided to use ProLine® over Hydrodarco® 3000 because it was less expensive. However, both adsorbents showed a similar level of absorption efficiency. In terms of the type of modification, heat-treated ProLine® was chosen due to its absorption efficiency and simplicity of the process. A pre-treatment with HCl acid followed by heat treatment also resulted in high absorption efficiency. Still, by

 

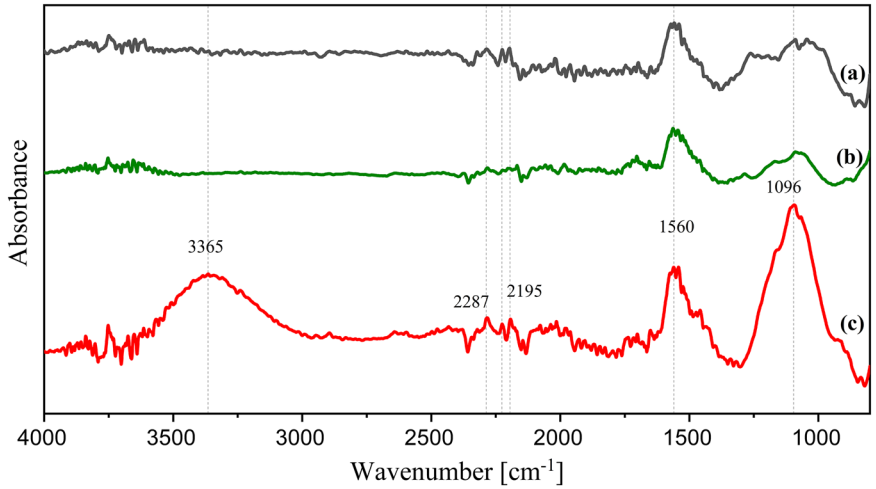


**Fig. 1** Typical FTIR spectra of (a) P, (b) $P_{HT}$ and (c) $P_{Cl,HT,HN}$.

eliminating the pre-treatment, the efficiency remains in the same range, and it is more economical from a cost perspective. Finally, larger particles were selected due to their ease of handling during the process and regeneration. Prior to discussing the adsorption isotherm and kinetics results, we examine the characteristics of the ProLine® before and after modification.

### 3.2. Characteristic of functionalized activated carbon

The GAC samples modified in the experimental section were used for FTIR, SEM, BET, and UV/vis spectra analysis. The results are shown in the following section.

**3.2.1. Chromophoric groups of samples.** To evaluate the surface functional groups present on the activated carbon, FTIR transmission spectra were conducted. Fig. 1 illustrates the FTIR spectra of untreated activated carbon (P) and functionalized samples ($P_{HT}$ and $P_{Cl,HT,HN}$) within the wavenumber range of 4000–800 $cm^{-1}$. Notably, three broad peaks were observed in the spectra of $P_{Cl,HT,HN}$.

An absorbance peak in the infrared range of 3600–3000 $cm^{-1}$, with its maximum at 3365 $cm^{-1}$, can be attributed to the vibrational stretch of hydroxyl groups (OH). This peak signifies the presence of O–H groups originating from alcohol compounds.[55,56] Another broad peak in the wavenumber range of 1300–950 $cm^{-1}$, with its maximum at 1096 $cm^{-1}$, was observed in the spectra of the oxidized activated carbon with nitric acid ($P_{Cl,HT,HN}$). This peak corresponds to the stretching of the C–O group, which can arise from alcohol, acids, ethers, and/or ester functional groups.[56] These findings align with previous literature, indicating that oxidation with $HNO_3$ increases the quantity of oxygen-containing functional groups on the activated carbon surface.[57–60]

The peak at 1560 $cm^{-1}$ observed in all spectra holds particular significance as it corresponds to the stretching vibration of C=C bonds present in aromatic ring structures.[61] Additionally, there are sharp, weak bands at approximately 2100 $cm^{-1}$ indicating carbon–carbon triple bonds, as well as peaks around 2250 $cm^{-1}$ resulting from carbon–nitrogen triple bonds.[62] It is worth noting that the fingerprint region of the infrared spectrum, spanning from 600 to 1400 $cm^{-1}$, is particularly complex, displaying numerous overlapping bands. While the entire IR spectrum can serve as a fingerprint for molecular comparison, this specific range is often referred to as the fingerprint region.[63]

**3.2.2. Morphological and texture of samples.** Fig. 2 presents SEM images comparing untreated activated carbon (P) with functionalized samples ($P_{HT}$ and $P_{Cl,HT,HN}$). The images reveal that the activated carbons exhibit a heterogeneous surface with randomly distributed pores. Two distinct surface morphologies are observed in the adsorbents: one resembling fibers and the other displaying an amorphous structure, referred to as the non-fiber zone.

The Fig. 2A shows a relatively smooth surface with tiny particles on the surface of as-received activated carbon (P). These particles might be assumed to be inorganic components or ashes. However, after the chain of treatments with HCl, heat treatment, and oxidation with $HNO_3$ ($P_{Cl,HT,HN}$), fewer fine particles could be found on the surface of the carbon (Fig. 2E). Those particles have disappeared partly due to HCl treatment. Besides, one can see that the walls around pores (Fig. 2E) become thinner than the as-received GAC (Fig. 2A), and newly created cavities on the surface of $P_{Cl,HT,HN}$ are apparent. These cavities were not seen on the surface of $P_{HT}$ (Fig. 2C); therefore, these differences could result from nitric acid treatment, which oxidized the surface of activated carbon. Similarly, in the fiber zone, a relatively smooth surface with many grooves, furrows, and tiny particles could be found in the P (Fig. 2B) and $P_{HT}$ (Fig. 2D) samples. On the other hand, in the fiber zone of $P_{Cl,HT,HN}$ (Fig. 2F), the walls became thinner, and the surface of the fibers became rougher compared to P and $P_{HT}$, because of the reaction of $HNO_3$ with AC's surface.

The main constituting elements of non-functionalized and functionalized activated carbon (AC) samples were analyzed

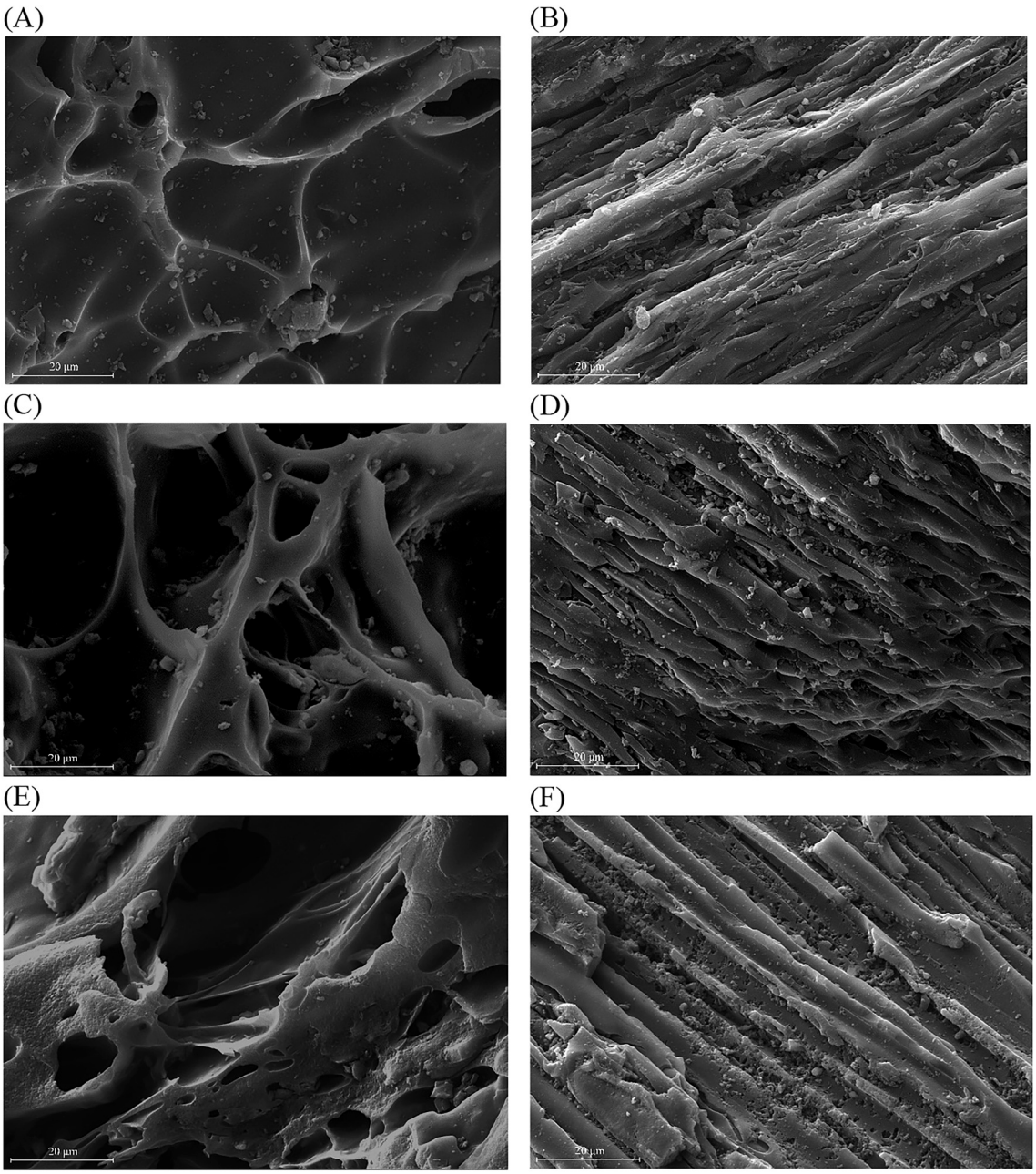


**Fig. 2** Typical SEM images of the samples, (A) P non-fiber zone, (B) P fiber zone, (C) $P_{HT}$ non-fiber zone, (D) $P_{HT}$ fiber zone, (E) $P_{Cl,HT,HN}$ non-fiber zone, and (F) $P_{Cl,HT,HN}$ fiber zone.

and quantified using SEM-EDS analyses, and the corresponding results are summarized in Table 4. The purpose of this analysis was to assess the changes in elemental composition induced by different treatments. Upon examining the results, it is evident that heat treatment under $N_2$ gas caused an expected decrease in the oxygen

**Table 4** SEM-EDS elemental contents of the ProLine® before and after modification

| Type of activated carbon | Elements | | | |
|---|---|---|---|---|
| | C (%) | O (%) | N (%) | Remaining (%) |
| P | 87.61 | 8.59 | 2.12 | 1.68 |
| $P_{HT}$ | 92.39 | 5.26 | 1.24 | 1.11 |
| $P_{Cl,HT,HN}$ | 77.32 | 18.56 | 3.90 | 0.22 |

**Table 5** Textural characteristics of the ProLine® before and after modification

| Sample | $S_{BET}$ [$m^2\ g^{-1}$] | Pore volume (<78 nm) [$cm^3\ g^{-1}$] | Average pore size [nm] |
|---|---|---|---|
| P | 767.05 | 0.5199 | 2.711 |
| $P_{HT}$ | 745.81 | 0.5053 | 2.710 |
| $P_{Cl,HT,HN}$ | 700.41 | 0.4703 | 2.686 |

 

content when compared to non-functionalized carbon (P). This reduction in oxygen content can be attributed to the high-temperature treatment, which likely facilitated the removal of oxygen-containing functional groups from the surface of the activated carbon. In contrast, when the activated carbon samples underwent oxidation with $HNO_3$ in the $P_{Cl,HT,HN}$ samples, the content of both oxygen and nitrogen increased. This observation suggests that the $HNO_3$ treatment introduced new oxygen and nitrogen functional groups onto the surface of the activated carbon. The nitric acid acted as an oxidizing agent, leading to the formation of oxygen-containing groups, such as carboxyl and hydroxyl groups, as well as nitrogen-containing groups, like amine and amide functionalities.[64]

**3.2.3. Specific surface.** Table 5 provides an overview of the textural characteristics of the activated carbon (ProLine®) before and after modification. Notably, the $HNO_3$-oxidized sample ($P_{Cl,HT,HN}$) exhibits minimal changes in surface area and pore volume. This observation can be attributed to the presence of oxygen-containing functional groups on the activated carbon surface. These groups may occupy certain surface sites, limiting access to a portion of the carbon surface and thus contributing to a slight decrease in surface area and pore volume. The SEM images also revealed the formation of new cavities on the surface of $P_{Cl,HT,HN}$. These cavities could potentially contribute to the marginal reduction in average pore size observed in the $P_{Cl,HT,HN}$ sample. Overall, these findings suggest that the modification process has a limited impact on the textural properties of the activated carbon, potentially due to the presence of oxygen-containing groups and the formation of surface cavities.

**3.2.4. Absorption and dispersion of light irradiations.** To evaluate the extent of dispersion of the surface-modified activated carbon in water, a UV/vis spectroscopy was used. A certain quantity of P, $P_{HT}$, and $P_{Cl,HT,HN}$ were dissolved in distilled water as a solvent to form the suspensions. Fig. 3 presents the transmittance of the solution in the wavelength range of 200 to 800 nm 24 h after sonication to ensure they were stable. The unmodified-AC, P, showed a transmittance of 72%. The hydrophilic nature of the activated carbon led to the dispersion of nanoparticle-activated carbon in water. The oxygen content of activated carbon contributes to its hydrophilicity.[65] A transmittance of 90% in the diagram of $P_{HT}$ indicated that the heat-treated sample was poorly dispersed in the solvent and precipitated out eventually. Heat treatment of activated carbon at high temperatures under a flow of nitrogen removed some surface groups, especially oxygenated groups.[64] The hydrophilicity of the carbon was reduced; consequently, the modified activated carbon, $P_{HT}$, was not appropriately dispersed in water. On the other hand, the lowest transmittance (~40%) was demonstrated by the $P_{Cl,HT,HN}$ samples, most likely due to the newly formed functional groups on the carbon surface. It was reported that the strong acids were used to modify AC, which resulted in the development of polar, hydrogen-bonding functional groups like carboxylic acid on the surface.[66] Therefore, hydrophilicity ascribed to the carboxylic groups developed on the surface of AC samples resulted in the solubility of $P_{Cl,HT,HN}$ in water.

Furthermore, given that the $P_{Cl,HT,HN}$ samples have a lower transmittance than the P, it can be deduced that the former has a higher level of functionalization efficiency. Fig. 4 shows a picture of the bottles containing the P, $P_{HT}$, and $P_{Cl,HT,HN}$ dispersions. It is visually evident that $P_{Cl,HT,HN}$ has a higher degree of dispersion in water, inferring the presence of functional groups on their surface.

### 3.3. Adsorption isotherms

Batch experiments were carried out to determine the equilibrium isotherm of contaminants. To this end, different amounts of $P_{HT}$ (heat treated AC (ProLine®) at 900 °C under nitrogen flow) was added to SLWW (from 0.36 to 10.00 g $L^{-1}$). Then the residual concentrations of $NPEO_{3-17}$ and COD in solution were measured. The adsorption capacity and

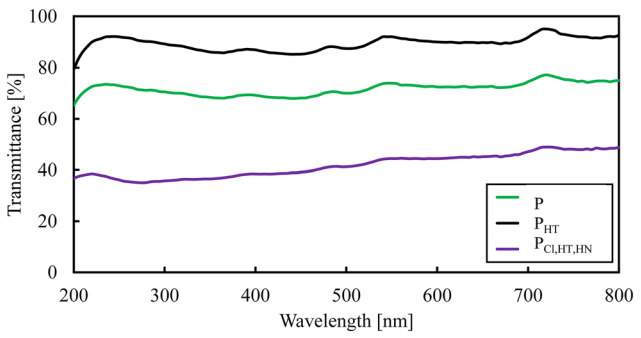


Fig. 3 Typical transmittance spectra of P, $P_{HT}$, and $P_{Cl,HT,HN}$ suspension samples after 24 h settlement time.

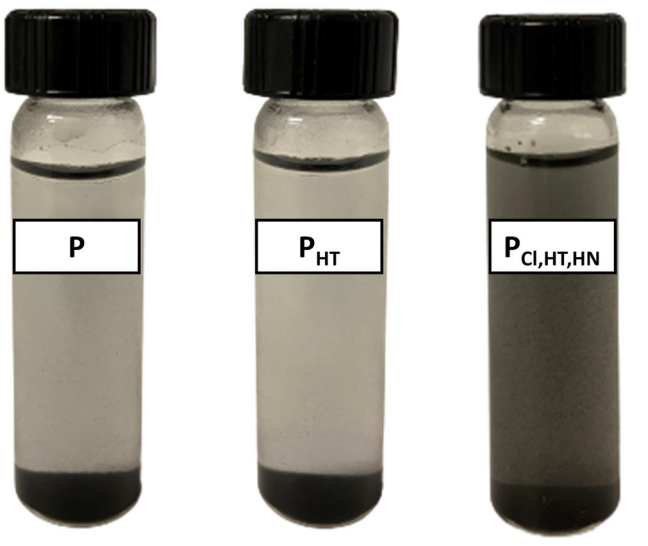


Fig. 4 Image of the P, $P_{HT}$, and $P_{Cl,HT,HN}$ suspensions in distilled water after 24 h settlement time.

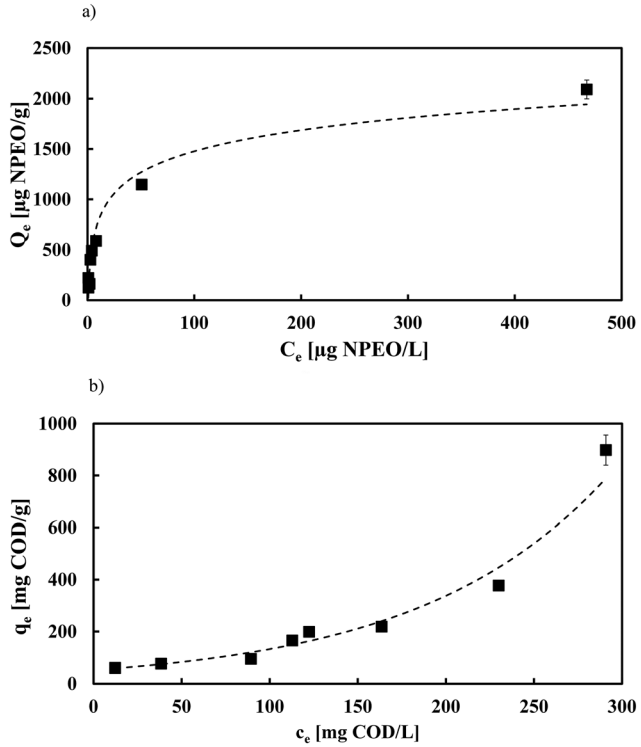


**Fig. 5** Adsorption isotherm of a) $NPEO_{3–17}$ and b) COD by $P_{HT}$ (conditions: initial $NPEO_{3–17}$ = 971.3 ± 93.5 µg $L^{-1}$, initial COD = 572.9 ± 55.0 mg $L^{-1}$, $T$ = 20 ± 2 °C, pH = 7.0 ± 0.5, shaker speed = 150 rpm, treatment time = 180 min).

removal efficiency were determined according to eqn (1) and (2). Fig. S1† shows the influence of $P_{HT}$ dose on the $NPEO_{3–17}$ removal percentage and adsorption capacity. As shown in Fig. S1,† the $NPEO_{3–17}$ removal efficiency achieved 99% when the $P_{HT}$ dose was 2.00 g $L^{-1}$. It is apparent that the adsorption efficiency rose by increasing the adsorbent dose. It is readily understood that the number of available adsorption sites increased by increasing the adsorbent dose, resulting in increased removal efficiency.

Nevertheless, by increasing the GAC dose, the adsorption capacity declined from 2090 µg $g^{-1}$ at 0.36 g $L^{-1}$ of $P_{HT}$ to 123 µg $g^{-1}$ at 10.00 g $L^{-1}$ of 600 mg $P_{HT}$. The adsorption capacity decreased while increasing adsorbent concentrations. This was attributed to the unsaturation of adsorption sites through the adsorption process.

Another reason may be the particle interaction, such as aggregation, resulting from high GAC concentration. Such aggregation would lead to a decrease in the total surface area of carbon particles available for adsorption and an increase in diffusional path length. Particle interaction may also desorb some sorbate that is only loosely and reversibly bound to the carbon surface.[67] The COD removal and adsorption capacity show the same trend as $NPEO_{3–17}$. By comparison to $NPEO_{3–17}$ removal, and as shown in Fig. S2,† the COD removal achieved 98% when the $P_{HT}$ concentration was 10.0 g $L^{-1}$.

Fig. 5a and b, respectively, illustrate the equilibrium curves for the adsorption of $NPEO_{3–17}$ and COD on $P_{HT}$ sorbents. According to the adsorption isotherm classification proposed by Giles *et al.* (1960),[41] the plot of $NPEO_{3–17}$ was L curves or normal isotherm. Initially, as adsorbate concentration increased, adsorbate found a site available until the number of adsorption sites was limited, leading to a plateau. On the other hand, the isotherm for COD was S curves or vertical orientation type. In type S isotherms, the adsorption behavior is opposite to that of type L, resulting in an increase in the slope of the curve with increasing adsorbate concentrations. At higher concentrations, the solute molecules had a tendency to orient vertically, thus providing more sites for adsorption.[41] Considering the shape of the upper parts of the curves, including plateax and changes in the slope, $NPEO_{3–17}$ and COD isotherms were placed in L2 and S1 subgroups, respectively. A subclass 2 of the L type isotherm means that the solutes had no intermolecular interactions, with a long plateau indicating a saturation of the adsorbent monolayer. Subclass 1 of the S type

**Table 6** Isotherm models and parameters for $NPEO_{3–17}$ adsorption on $P_{HT}$ (conditions: initial $NPEO_{3–17}$ = 971.3 ± 93.5 µg $L^{-1}$, $T$ = 20 ± 2 °C, pH = 7.0 ± 0.5, shaker speed = 150 rpm, treatment time = 180 min)

| Isotherm model | Expression | Parameter | Goodness of fit |
|---|---|---|---|
| Langmuir | $Q_e = \frac{Q_m K_a C_e}{1 + K_a C_e}$ | $Q_m$ = 2168.3 µg $g^{-1}$ | $R^2$ = 0.995 |
| | $\frac{C_e}{Q_e} = \frac{1}{Q_m} C_e + \frac{1}{K_a Q_m}$ | $K_a$ = 0.0506 L $\mu g^{-1}$ | |
| Temkin | $Q_e = \beta \ln(K_t C_e)$ | $\beta$ = 302.4 µg $g^{-1}$<br>$K_t$ = 1.3242 L $\mu g^{-1}$ | $R^2$ = 0.963 |
| Freundlich | $Q_e = K_f C_e^{1/n}$ | $K_f$ = 266.4 $\mu g^{0.6612}$ $L^{0.3388}$ $g^{-1}$<br>$n$ = 2.95 | $R^2$ = 0.974 |
| Redlich–Peterson | $Q_e = \frac{K_r C_e}{1 + A_r C_e^{\beta}}$ | $K_r$ = 274.6 L $g^{-1}$<br>$A_r$ = 0.5468 L $\mu g^{-1}$<br>$\beta$ = 0.7655 | $R^2$ = 0.990 |
| Liu | $Q_e = \frac{Q_m (K_a C_e)^{n_g}}{1 + (K_a C_e)^{n_g}}$ | $Q_m$ = 3095.3 µg $g^{-1}$<br>$K_g$ = 0.0080 L $\mu g^{-1}$<br>$n_g$ = 0.55 | $R^2$ = 0.988 |

 

**Table 7** Isotherm models and parameters for COD adsorption on $P_{HT}$ (conditions: initial COD = 572.9 ± 55.0 mg $L^{-1}$, $T$ = 20 ± 2 °C, pH = 7.0 ± 0.5, shaker speed = 150 rpm, treatment time = 180 min)

| Isotherm model | Expression | Parameter | Goodness of fit |
|---|---|---|---|
| Langmuir | $q_e = \frac{q_m K_a c_e}{1 + K_a c_e}$ | $q_m$ = 235.1 mg $g^{-1}$ | $R^2$ = 0.695 |
| | $\frac{1}{q_e} = \frac{1}{q_m K_a}\frac{1}{c_e} + \frac{1}{q_m}$ | $K_a$ = 0.0255 L $mg^{-1}$ | |
| Temkin | $q_e = \beta \ln(K_t c_e)$ | $\beta$ = 181.4 mg $g^{-1}$<br>$K_t$ = 0.0447 L $mg^{-1}$ | $R^2$ = 0.456 |
| Freundlich | $q_e = K_f c_e^{1/n}$ | $K_f$ = 0.0036 $L^{2.176}$ $mg^{-1.176}$ $g^{-1}$<br>$n$ = 0.46 | $R^2$ = 0.929 |
| Redlich–Peterson | $q_e = \frac{K_r c_e}{1 + A_r c_e^{\beta}}$ | $K_r$ = 4.204 × $10^4$ L $g^{-1}$<br>$A_r$ = 3.349 × $10^5$ L $mg^{-1}$<br>$\beta$ = −0.5342 | $R^2$ = 0.892 |
| Liu | $q_e = \frac{q_m (K_a c_e)^{n_g}}{1 + (K_a c_e)^{n_g}}$ | $q_m$ = 5.229 × $10^4$ mg $g^{-1}$<br>$K_g$ = 0.0003 L $mg^{-1}$<br>$n_g$ = 1.61 | $R^2$ = 0.899 |

isotherm shows a complete vertical behavior of the adsorption capacity.[68]

To better understand the relationship between the capacity of the adsorbent and targeted pollutants, different adsorption isotherm models were used: Langmuir, Temkin, Freundlich, Redlich–Peterson, and Liu models. The results are presented in Tables 6 and 7 for $NPEO_{3-17}$ and COD, respectively. Among these equilibrium models, Langmuir isotherm described better the adsorption process (with an $R^2$ value as high as 0.995) over the entire $NPEO_{3-17}$ concentration range studied (971.3 ± 93.5 μg $NPEO_{3-17}$ per L) (Table 6). Indeed, Langmuir adsorption isotherm is valid for monolayer sorption on a surface containing a limited number of sites, predicting a homogenous distribution of sorption energy.[69] The maximum $NPEO_{3-17}$ concentration ($Q_m$) capable of being adsorbed on $P_{HT}$ sorbent was estimated to be 2.17 mg $g^{-1}$.

This $Q_m$ value of $NPEO_{3-17}$ calculated according to the Langmuir equation can be compared with other adsorbents reported in the literature. Del Bubba *et al.* (2020)[70] studied the sorption capacities of sawdust-based biochars, pyrolyzed at 450, 650, and 850 °C (BC450, BC650, and BC850), and commercial activated carbons towards NPEO in textile wastewater. The maximum 4-$NP_8EO$ concentrations capable of adsorbing on these adsorbents were estimated to be 1.67 ± 0.09 mg $g^{-1}$ (for sawdust-based biochars, BC850) and 20.2 ± 0.3 mg $g^{-1}$ (for commercial activated carbons). In another study, the effect of the initial concentration of $NP_9EO$ was evaluated in the maximum adsorption capacity on a crosslinked β-cyclodextrin-carboxymethylcellulose (β-CD-CMC) polymer. The maximum $NP_9EO$ concentration capable of adsorbing on β-CD-CMC adsorbent was estimated to increase from 1.10 ± 0.01 to 6.8 ± 0.1 mg $g^{-1}$, while the initial concentration of $NP_9EO$ in the effluent increased from 12 to 82 mg $L^{-1}$.[71] It is worth noting that the initial concentration of the effluent is one of the main factors on the adsorption capacity.

Considering the equilibrium curve of COD removal (Table 7), Freundlich equations described very well the adsorption (with an $R^2$ value of 0.929 for the best fit) over the entire sorbent concentration range studied (*i.e.*; 572.9 ± 55.0 mg COD per L). Freundlich equation assumes that there are multiple types of sorption sites acting in parallel, each site exhibiting a different sorption free energy. For the Freundlich constant $n > 1$, the sorbates are bound with weaker and weaker free energies. By comparison, when $n < 1$, it indicates that the free energy can be enhanced and more sorbate can be adsorbed on the sorbent.[69] In the present study, $n$ = 0.45 (see Table 7), it means that more COD can be adsorbed on $P_{HT}$ sorbent. By comparison, Ahmad and Hameed (2009)[72] reported that adsorption of COD from textile wastewater onto the activated carbon prepared from bamboo waste was well described by Freundlich isotherm and the value of n was closed to 3.1. On the other hand, Patel (2022)[73] investigated the adsorption of COD from distillery spent wash using bagasse fly ash as the sorbent. In their study, they obtained a Freundlich exponent, $n$, of 0.66, indicating a different adsorption behavior compared to the previous research. These findings highlight the influence of experimental conditions on the adsorption process, indicating that factors such as sorbent type and wastewater composition can significantly influence the adsorption mechanism. Overall, these data emphasize the importance of considering the

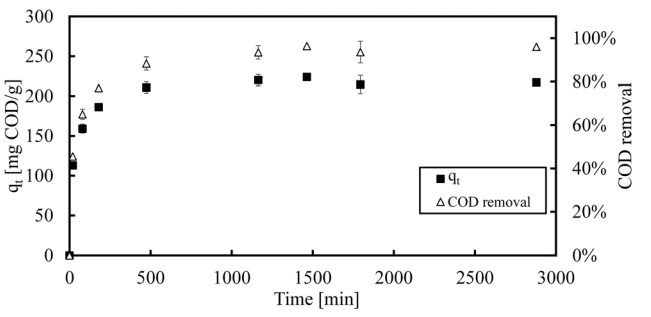


**Fig. 6** Adsorption kinetics of COD on $P_{HT}$ (conditions: initial COD = 572.9 ± 55.0 mg $L^{-1}$, $T$ = 20 ± 2 °C, pH = 7.0 ± 0.5, shaker speed = 150 rpm, treatment time = 48 h).

Table 8 Kinetic models and parameters for COD adsorption on $P_{HT}$ (conditions: initial COD = 572.9 ± 55.0 mg $L^{-1}$, $T$ = 20 ± 2 °C, pH = 7.0 ± 0.5, shaker speed = 150 rpm, treatment time = 48 h)

| Kinetic model | Expression | Parameter | Goodness of fit |
|---|---|---|---|
| Pseudo-first-order model | $q_t = q_e(1 - e^{k_{p1}t})$ | $q_e$ = 209.9 mg $g^{-1}$<br>$k_{p1}$= 0.0277 $min^{-1}$ | $R^2$ = 0.950 |
| Pseudo-second-order model | $q_t = \frac{k_{p2}q_e^2 t}{1 + k_{p2}q_e t}$ | $q_e$ = 219.3 mg $g^{-1}$<br>$k_{p2}$ = 0.0002 g $mg^{-1}$ $min^{-1}$ | $R^2$ = 0.982 |
| Elovich model | $q_t = \frac{1}{\alpha}\ln(1 + \alpha\beta t)$ | $\alpha$ = 0.0469 g $mg^{-1}$<br>$\beta$ = 420.0 mg $g^{-1}$ $min^{-1}$ | $R^2$ = 0.993 |
| Second-order rate model | $\frac{1}{c_t} = k_2 t + \frac{1}{c_e}$ | $k_2$ = 1.042 × $10^{-5}$ L $mg^{-1}$ $min^{-1}$<br>$c_e$ = 185.9 mg $L^{-1}$ | $R^2$ = 0.799 |
| Intraparticle diffusion | $q_t = k_p t^{1/2} + I$ | $k_p$ = 3.041 mg $g^{-1}$ $min^{-0.5}$<br>$I$ = 98.3 mg $g^{-1}$ | $R^2$ = 0.596 |

specific experimental conditions and characteristics of the adsorbent and wastewater when studying adsorption processes. The variations in the Freundlich exponent, $n$, indicate that adsorption behavior can differ depending on the experimental setup and underline the need for comprehensive investigations to gain a better understanding of the adsorption mechanisms under various conditions.

### 3.4. Adsorption kinetics

A kinetic study is valuable for determining the contact time between adsorbent and adsorbate, controlling the efficiency of the process and understanding the mechanisms of the sorption process. Fig. 6 shows the removal of COD by $P_{HT}$ against time. Results showed that the COD removal reached 90% after 8 h, and the efficiency increased gradually to reach 96% after 48 h. The adsorption rate was initially rapid, probably due to a large number of free surface sites available on $P_{HT}$ sorbents. Afterward, the adsorption rate became slower.

The adsorption of COD through activated carbon can be described in three phases based on the nature of the removal curves in Fig. 6. During the first phase (0–20 min), the adsorption process of COD onto the adsorbent material was found to be instantaneous and faster. This phase is referred to as external surface diffusion. In this stage, the adsorbent material, which in this case is $P_{HT}$, had an ample number of active adsorption sites available for the pollutant to attach to. As a result, the adsorption process occurred rapidly. Moving into the second phase (20–470 min), gradual adoption of COD was observed. This suggests that the adsorption mechanism during this phase is primarily governed by intra-particle diffusion. Intra-particle diffusion attributed to the inter-ionic attraction and molecular interaction between the adsorbent's active sites and the adsorbate. As time progresses further into the second phase, the concentration of COD gradually decreases due to the ongoing adsorption process. The decrease in available active sites on the adsorbent leads to a slower rate of adsorption. This is because the adsorbent's active sites are gradually being occupied by COD molecules, limiting the surface area available for further adsorption. In the final phase (470–2880 min), adsorption reaches equilibrium. At this stage, the concentration of COD in the solution becomes stable. The active sites on the adsorbent may have started to decrease during this phase, contributing to the slower adsorption rate observed.[74]

Adsorption kinetic allows an understanding of the mechanism of the sorption process for COD removal. To evaluate the sorption rate, the kinetic data were modeled using pseudo-first order and pseudo-second order equations. Elovich model[44] and diffusional mass transfer (intra-particle diffusion model) have been also applied. The data are summarized in Table 8. High correlation coefficients were obtained for pseudo-second-order ($R^2$ = 0.982) and Elovich ($R^2$ = 0.993) kinetic models. However, Elovich equation fitted the data better than the pseudo-second equation. The Elovich constant, $\alpha$, and the initial adsorption rate, $\beta$, were obtained 0.0469 g $mg^{-1}$ and 420.04 mg $g^{-1}$ $min^{-1}$, respectively.

In the study conducted by Rubi-Juarez *et al.* (2017),[75] they examined the adsorption of COD in carwash wastewater using commercial granular activated carbon at different concentrations of 7.5, 15, and 22.5 g $L^{-1}$. The researchers observed a decrease in the initial adsorption rate, which decreased from 24.197 to 8.780 mg $g^{-1}$ $min^{-1}$ as the concentration of activated carbon was reduced. In another investigation focused on COD adsorption kinetics, various adsorbents were employed. The results showed distinct initial

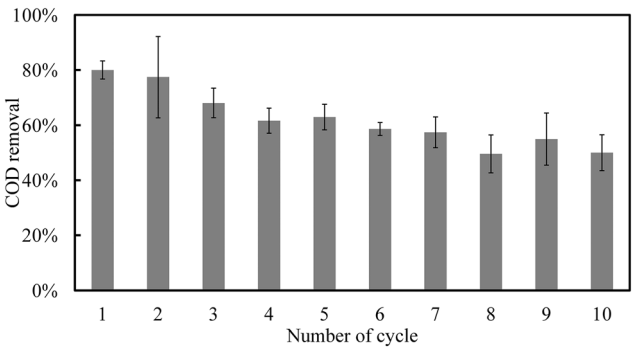


Fig. 7 Effect of the number of adsorption cycles on the COD removal on $P_{HT}$ (conditions: initial $NPEO_{3-17}$ = 971.3 ± 93.5 μg $L^{-1}$, initial COD = 572.9 ± 55.0 mg $L^{-1}$, $T$ = 20 ± 2 °C, pH = 7.0 ± 0.5, shaker speed = 150 rpm, treatment time = 180 min).

 

adsorption rates for each adsorbent. For activated carbon, the initial adsorption rate was found to be 1.53 mg $g^{-1}$ $min^{-1}$, while zeolite exhibited a significantly higher initial adsorption rate of 505.37 mg $g^{-1}$ $min^{-1}$. Composite materials demonstrated the highest initial adsorption rate, measuring at $1.34 \times 10^4$ mg $g^{-1}$ $min^{-1}$. Additionally, the Elovich constant, which indicates the desorption constant, was determined for the mentioned adsorbents. The values recorded were 0.1407 g $mg^{-1}$ for activated carbon, 1.2582 g $mg^{-1}$ for zeolite, and 0.7330 g $mg^{-1}$ for composite materials.[76] These findings highlight the variations in the adsorption kinetics and Elovich constants among different adsorbents. The observed differences emphasize the influence of the choice of adsorbent material on the adsorption process and suggest the importance of selecting the appropriate adsorbent based on the specific application and target pollutant.

Elovich equation is applied to determine the kinetics of the chemisorption process.[68] The COD adsorption in our study is probably governed by chemisorption processes. To be sure about this statement, the energy of adsorption should be measured based on the thermodynamics of adsorption. Chemisorption involves chemical bonding and electron transfer between adsorbents and adsorbates. Interactions are mediated mainly by ionic or covalent bonds.[33]

### 3.5. Number of the adsorption cycles

Fig. 7 shows the effect of the number of adsorption cycles on the removal efficiency of $P_{HT}$. It was found that the COD removal percentage reduced from 80% to 50%, whereas $NPEO_{3-17}$ efficiency reduced from 99.6% to 95.9% after ten consecutive adsorption cycles. The results indicated that the used samples remain reactive with sufficient removal efficiencies of surfactant molecules with multiple cycles. Hence, the activated carbon still contains free and available active sites to adsorb more contaminants. After the regeneration of the spent adsorbent ($P_{HT}$), the activated carbon was again employed to remove COD and $NPEO_{3-17}$. The efficiency was obtained at 85% of the original for COD and 100% of the fresh $P_{HT}$ for $NPEO_{3-17}$ removal.

## 4. Conclusion

In this study, we used multistep modification methods on different coal-based GAC to observe the effect of these modifications on their removal efficiency of $NPEO_{3-17}$ in the adsorption process. Functionalizing GAC aims to enhance the activated carbon capacity to remove $NPEO_{3-17}$ and COD from the synthetic wastewater. The modification process included acid treatment with HCl to remove the inorganic contaminants, heat treatment under nitrogen gas at 900 °C to eliminate oxygen-acidic surface groups, and acid treatment with $HNO_3$ to introduce oxygen functional groups.

By using heat treatment, the adsorption capacity of activated carbon increased remarkably in comparison with acid treatment using $HNO_3$. In a batch adsorption process, the percentages of COD removal using P, $P_{HT}$ and $P_{Cl,HT,HN}$, samples were 63%, 80%, and 56%, respectively. The initial COD was 572.9 ± 55.0 mg $L^{-1}$ in synthetic laundry wastewater. By comparison, the percentages of $NPEO_{3-17}$ removal were 99.55%, 99.54%, and 94.46%, respectively. The initial $NPEO_{3-17}$ concentration was 971.3 ± 93.5 μg $L^{-1}$.

The experiments were then performed by using a relatively low concentrations of the activated carbon 0.37 g $L^{-1}$. In these conditions, $NPEO_{3-17}$ removal efficiencies of 41% and 62% were recorded while using untreated sorbent (P) and modified sorbent ($P_{HT}$), respectively. Likewise, $NPEO_{3-17}$ adsorption capacities of 550 and 2092 μg $g^{-1}$ were measured for P and $P_{HT,}$ respectively. It is worth noting that the pretreatment of activated carbon contributes to increase the adsorption capacity by 35% (for $NPEO_{3-17}$ removal). The proposed thermal treatment of AC successfully enhanced their removal capacity of COD and $NPEO_{3-17}$ by 17% and 21%, respectively.

## List of abbreviation

| | |
|---|---|
| AC | Activated carbon |
| $AC_{Cl}$ | Modified activated carbon with hydrochloric acid |
| $AC_{HN}$ | Functionalized activated carbon with nitric acid |
| $AC_{HT}$ | Heat-treated activated carbon under $N_2$ gas |
| AOPs | Advanced oxidation processes |
| APEO | Alkylphenol ethoxylate |
| BET | Brunauer–Emmett–Teller |
| BJH | Barrett–Joyner–Halenda |
| CMC | Critical micelle concentration |
| COD | Chemical oxygen demand |
| EDS | Energy dispersive X-ray spectrometry |
| EO | Ethoxylated groups |
| EPA | Environmental protection agencies |
| F400 | FILTRASORB® 400 |
| FTIR | Fourier transform infrared |
| GAC | Granular activated carbons |
| HD | HYDRODARCO® 3000 |
| LWW | Laundry wastewater |
| MN100 | Macronet™ MN100 |
| MN200 | Macronet™ MN200 |
| NP | Nonylphenol |
| NPEO | Nonylphenol ethoxylates |
| OPEO | Octylphenol ethoxylates |
| OP | Octylphenol |
| P | ProLine® |
| *R* | Removal efficiency |
| $R^2$ | Regression coefficient |
| RE | Regeneration efficiency |
| SEM | Scanning electron microscopy |
| SLWW | Synthetic laundry wastewater |

## Author contributions

Mahdieh Khajvand: conceptualization, investigation, visualization, methodology, writing – original draft. Patrick Drogui: conceptualization, supervision, funding acquisition,

methodology, writing – review & editing. Loick Pichon: investigation, writing – review & editing. My Ali El Khakani: investigation, writing – review & editing. Rajeshwar Dayal Tyagi: writing – review & editing. Emmanuel Brien: funding acquisition, writing – review & editing.

## Conflicts of interest

The authors declare that they have no known competing financial interests or personal relationships that could have appeared to influence the work reported in this paper.

## Acknowledgements

The authors are grateful to the National Sciences and Engineering Research Council of Canada, the Group VEOS, and to the CREATE TEDGIEER program for their financial support.

## References

1 M. Badea, C. Nistor, Y. Goda, S. Fujimoto, S. Dosho, A. Danet, D. Barceló, F. Ventura and J. Emnéus, A flow immunoassay for alkylphenol ethoxylate surfactants and their metabolites—questions associated with cross-reactivity, matrix effects, and validation by chromatographic techniques, *Analyst*, 2003, **128**, 849–856.
2 C. C. Borghi and M. Fabbri, Magnetic recovery of modified activated carbon powder used for removal of endocrine disruptors present in water, *Environ. Technol.*, 2014, **35**, 1018–1026.
3 C. A. Staples, C. G. Naylor, J. B. Williams and W. E. Gledhill, Ultimate biodegradation of alkylphenol ethoxylate surfactants and their biodegradation intermediates, *Environ. Toxicol. Chem.*, 2001, **20**, 2450–2455.
4 M. Castillo, E. Martínez, A. Ginebreda, L. Tirapu and D. Barceló, Determination of non-ionic surfactants and polar degradation products in influent and effluent water samples and sludges of sewage treatment plants by a generic solid-phase extraction protocol, *Analyst*, 2000, **125**, 1733–1739.
5 A. A. Siyal, M. R. Shamsuddin, A. Low and N. E. Rabat, A review on recent developments in the adsorption of surfactants from wastewater, *J. Environ. Manage.*, 2020, **254**, 109797.
6 C. Werme, Alkylphenols and Alkylphenol Ethoxylates, **https://www.sfei.org/sites/default/files/general_content/APE_profile_0.pdf**).
7 Y. Patiño, E. Díaz, M. J. Lobo-Castañón and S. Ordóñez, Carbon nanotube modified glassy carbon electrode for electrochemical oxidation of alkylphenol ethoxylate, *Water Sci. Technol.*, 2018, **77**, 2436–2444.
8 A. Priac, N. Morin-Crini, C. Druart, S. Gavoille, C. Bradu, C. Lagarrigue, G. Torri, P. Winterton and G. Crini, Alkylphenol and alkylphenol polyethoxylates in water and wastewater: A review of options for their elimination, *Arabian J. Chem.*, 2017, **10**, S3749–S3773.
9 P. Kumari and A. Kumar, ADVANCED OXIDATION PROCESS: A remediation technique for organic and non-biodegradable pollutant, *Surf. Interfaces*, 2023, 100122.
10 D. Dutta, S. Arya and S. Kumar, Industrial wastewater treatment: Current trends, bottlenecks, and best practices, *Chemosphere*, 2021, **285**, 131245.
11 F. Thomas, J. Bottero, S. Partyka and D. Cot, Contribution of microcalorimetry to the study of adsorption mechanisms of ionic and non-ionic molecules at the solid-water interface, *Thermochim. Acta*, 1987, **122**, 197–207.
12 S. Murai, S. Imajo, Y. Maki, K. Takahashi and K. Hattori, Adsorption and recovery of nonionic surfactants by β-cyclodextrin polymer, *J. Colloid Interface Sci.*, 1996, **183**, 118–123.
13 N. Nikolenko, A. Korpach and Z. Masyuta, Adsorption of ethoxylated alkyl phenols on silica gel from aqueous micellar solutions, *Colloid J.*, 2002, **64**, 355–358.
14 W.-B. Yang and L. Ren, Adsorption mechanism of nonylphenol polyethoxylate onto hypercrosslinked resins, *Acta Phys.-Chim. Sin.*, 2010, **26**, 2182–2188.
15 J. Fan, W. Yang and A. Li, Adsorption of phenol, bisphenol A and nonylphenol ethoxylates onto hypercrosslinked and aminated adsorbents, *React. Funct. Polym.*, 2011, **71**, 994–1000.
16 A. K. Mostafazadeh, A. T. Benguit, A. Carabin, P. Drogui and E. Brien, Development of combined membrane filtration, electrochemical technologies, and adsorption processes for treatment and reuse of laundry wastewater and removal of nonylphenol ethoxylates as surfactants, *J. Water Process. Eng.*, 2019, **28**, 277–292.
17 P.-D. Nguyen, T.-M.-T. Le, T.-K.-Q. Vo, P.-T. Nguyen, T.-D.-H. Vo, B.-T. Dang, N.-T. Son, D. D. Nguyen and X.-T. Bui, Submerged membrane filtration process coupled with powdered activated carbon for nonylphenol ethoxylates removal, *Water Sci. Technol.*, 2021, **84**, 1793–1803.
18 O. Čižmárová, B. Urminská, J. Derco, A. Kassai and R. Zakhar, Removal of alkylphenols from industrial wastewater by means of ozone-based processes and fenton reaction, *Chem. Pap.*, 2021, 1–9.
19 M. C. Collivignarelli, M. C. Miino, M. Baldi, S. Manzi, A. Abbà and G. Bertanza, Removal of non-ionic and anionic surfactants from real laundry wastewater by means of a full-scale treatment system, *Process Saf. Environ. Prot.*, 2019, **132**, 105–115.
20 I. Ciabattia, F. Cesaro, L. Faralli, E. Fatarella and F. Tognotti, Demonstration of a treatment system for purification and reuse of laundry wastewater, *Desalination*, 2009, **245**, 451–459.
21 Q. Gao, W. Chen, Y. Chen, D. Werner, G. Cornelissen, B. Xing, S. Tao and X. Wang, Surfactant removal with multiwalled carbon nanotubes, *Water Res.*, 2016, **106**, 531–538.
22 P. Prediger, T. Cheminski, T. de Figueiredo Neves, W. B. Nunes, L. Sabino, C. S. F. Picone, R. L. Oliveira and C. R. D. Correia, Graphene oxide nanomaterials for the removal of

 

non-ionic surfactant from water, *J. Environ. Chem. Eng.*, 2018, **6**, 1536–1545.
23 P. Punyapalakul and S. Takizawa, Adsorption and recovery of alkylphenol polyethoxylates from synthetic wastewater using hexagonal mesoporous silicate, *Water Sci. Technol.*, 2006, **53**, 137–143.
24 A. Bhatnagar, W. Hogland, M. Marques and M. Sillanpää, An overview of the modification methods of activated carbon for its water treatment applications, *Chem. Eng. J.*, 2013, **219**, 499–511.
25 M. Soria-Sánchez, A. Maroto-Valiente, A. Guerrero-Ruiz and D. Nevskaia, Adsorption of non-ionic surfactants on hydrophobic and hydrophilic carbon surfaces, *J. Colloid Interface Sci.*, 2010, **343**, 194–199.
26 L. H. Leal, H. Temmink, G. Zeeman and C. Buisman, Characterization and anaerobic biodegradability of grey water, *Desalination*, 2011, **270**, 111–115.
27 S. H. Lin and H. G. Leu, Operating characteristics and kinetic studies of surfactant wastewater treatment by Fenton oxidation, *Water Res.*, 1999, **33**, 1735–1741.
28 S. Hazourli, M. Ziati and A. Hazourli, Characterization of activated carbon prepared from lignocellulosic natural residue:-Example of date stones, *Phys. Procedia*, 2009, **2**, 1039–1043.
29 M. Ahiduzzaman and A. S. Islam, Preparation of porous bio-char and activated carbon from rice husk by leaching ash and chemical activation, *Springerplus*, 2016, **5**, 1–14.
30 K. Chaillou, C. Gérente, Y. Andrès and D. Wolbert, Bathroom greywater characterization and potential treatments for reuse, *Water, Air, Soil Pollut.*, 2011, **215**, 31–42.
31 G. McKay and B. Al Duri, Multicomponent dye adsorption onto carbon using a solid diffusion mass-transfer model, *Ind. Eng. Chem. Res.*, 1991, **30**, 385–395.
32 Y. Matsui, A. Yuasa and F.-S. Li, Overall adsorption isotherm of natural organic matter, *J. Environ. Eng.*, 1998, **124**, 1099–1107.
33 M. Khajvand, A. K. Mostafazadeh, P. Drogui, R. D. Tyagi and E. Brien, Greywater characteristics, impacts, treatment, and reclamation using adsorption processes towards the circular economy, *Environ. Sci. Pollut. Res.*, 2022, 1–38.
34 L. Hernández-Leal, H. Temmink, G. Zeeman and C. Buisman, Removal of micropollutants from aerobically treated grey water via ozone and activated carbon, *Water Res.*, 2011, **45**, 2887–2896.
35 M. A. Tony, H. L. Parker and J. H. Clark, Evaluating Algibon adsorbent and adsorption kinetics for launderette water treatment: towards sustainable water management, *Water Environ. J.*, 2019, **33**, 401–408.
36 I. Langmuir, The adsorption of gases on plane surfaces of glass, mica and platinum, *J. Am. Chem. Soc.*, 1918, **40**, 1361–1403.
37 M. Temkin and V. Pyzhev, Kinetics of ammonia synthesis on promoted iron catalyst, *Acta Phys. Chim. USSR*, 1940, **12**, 327–356.
38 H. Freundlich, Over the adsorption in solution, *J. Phys. Chem.*, 1906, **57**, 1100–1107.
39 O. Redlich and D. L. Peterson, A useful adsorption isotherm, *J. Phys. Chem.*, 1959, **63**, 1024–1024.
40 Y. Liu and H. Xu, Equilibrium, thermodynamics and mechanisms of Ni2+ biosorption by aerobic granules, *Biochem. Eng. J.*, 2007, **35**, 174–182.
41 C. Giles, T. MacEwan, S. Nakhwa and D. Smith, 786. Studies in adsorption. Part XI. A system of classification of solution adsorption isotherms, and its use in diagnosis of adsorption mechanisms and in measurement of specific surface areas of solids, *J. Chem. Soc.*, 1960, 3973–3993.
42 S. K. Lagergren, About the theory of so-called adsorption of soluble substances, *Sven. Vetenskapsakad. Handingarl.*, 1898, **24**, 1–39.
43 Y.-S. Ho and G. McKay, Kinetic models for the sorption of dye from aqueous solution by wood, *Process Saf. Environ. Prot.*, 1998, **76**, 183–191.
44 I. McLintock, The Elovich equation in chemisorption kinetics, *Nature*, 1967, **216**, 1204–1205.
45 H. Qiu, L. Lv, B.-C. Pan, Q.-J. Zhang, W.-M. Zhang and Q.-X. Zhang, Critical review in adsorption kinetic models, *J. Zhejiang Univ., Sci., A*, 2009, **10**, 716–724.
46 W. J. Weber Jr and J. C. Morris, Kinetics of adsorption on carbon from solution, *J. Sanit. Eng. Div., Am. Soc. Civ. Eng.*, 1963, **89**, 31–59.
47 M. Mokhtarifar, H. Arab, M. Maghrebi and M. Baniadam, Amine-functionalization of carbon nanotubes assisted by electrochemical generation of chlorine, *Appl. Phys. A: Mater. Sci. Process.*, 2018, **124**, 1–9.
48 M. Greenbank and J. Knepper, GAC/PAC: Use of Powdered Activated Carbon for Potable Water Treatment in Small Systems, *Water Conditioning and Purification International*, 2002, pp. 44–51.
49 W. Xing, S. Zhuo, X. Gao and X. Yuan, Adsorption behavior of NPE on ordered mesoporous carbons, *Acta Chim. Sin.*, 2009, **67**, 1771–1778.
50 N. Querejeta, M. G. Plaza, F. Rubiera and C. Pevida, Water vapor adsorption on biomass based carbons under post-combustion CO2 capture conditions: Effect of post-treatment, *Materials*, 2016, **9**, 359.
51 P. Faria, J. Orfao and M. Pereira, Adsorption of anionic and cationic dyes on activated carbons with different surface chemistries, *Water Res.*, 2004, **38**, 2043–2052.
52 Y. Gokce and Z. Aktas, Nitric acid modification of activated carbon produced from waste tea and adsorption of methylene blue and phenol, *Appl. Surf. Sci.*, 2014, **313**, 352–359.
53 M. S. Shafeeyan, W. M. A. W. Daud, A. Houshmand and A. Shamiri, A review on surface modification of activated carbon for carbon dioxide adsorption, *J. Anal. Appl. Pyrolysis*, 2010, **89**, 143–151.
54 E. Calvo, R. Bravo, A. Amigo and J. Gracia-Fadrique, Dynamic surface tension, critical micelle concentration, and activity coefficients of aqueous solutions of nonyl phenol ethoxylates, *Fluid Phase Equilib.*, 2009, **282**, 14–19.
55 Z. Al-Qodah and R. Shawabkah, Production and characterization of granular activated carbon from activated sludge, *Braz. J. Chem. Eng.*, 2009, **26**, 127–136.
56 R. Ali, Z. Aslam, R. A. Shawabkeh, A. Asghar and I. A. Hussein, BET, FTIR, and RAMAN characterizations of

activated carbon from waste oil fly ash, *Turk. J. Chem.*, 2020, **44**, 279–295.

57 C. Yu, X. Fan, L. Yu, T. J. Bandosz, Z. Zhao and J. Qiu, Adsorptive removal of thiophenic compounds from oils by activated carbon modified with concentrated nitric acid, *Energy Fuels*, 2013, **27**, 1499–1505.

58 Z. Wang, E. Nie, J. Li, M. Yang, Y. Zhao, X. Luo and Z. Zheng, Equilibrium and kinetics of adsorption of phosphate onto iron-doped activated carbon, *Environ. Sci. Pollut. Res.*, 2012, **19**, 2908–2917.

59 G. Zolfaghari, A. Esmaili-Sari, H. Younesi and R. R. Baydokhti, Surface modification of ordered nanoporous carbons CMK-3 via a chemical oxidation approach and its application in removal of lead pollution from water, *Science and Technology, IPCBEE*, 2011, **6**, 174–178.

60 S. A. Dastgheib, T. Karanfil and W. Cheng, Tailoring activated carbons for enhanced removal of natural organic matter from natural waters, *Carbon*, 2004, **42**, 547–557.

61 K. J. Lee, J. Miyawaki, N. Shiratori, S.-H. Yoon and J. Jang, Toward an effective adsorbent for polar pollutants: Formaldehyde adsorption by activated carbon, *J. Hazard. Mater.*, 2013, **260**, 82–88.

62 S. Cortes, 10.7: Functional Groups and IR Tables, **https://chem.libretexts.org/Ancillary_Materials/Laboratory_Experiments/Wet_Lab_Experiments/Organic_Chemistry_Labs/Lab_I/10%3A_Infrared_Spectroscopy/10.07%3A_Functional_Groups_and_IR_Tables**).

63 J. Beauchamp, Infrared Tables (short summary of common absorption frequencies), *Course Notes*, 2010, **2620**, 19.

64 P. Treeweranuwat, P. Boonyoung, M. Chareonpanich and K. Nueangnoraj, Role of nitrogen on the porosity, surface, and electrochemical characteristics of activated carbon, *ACS Omega*, 2020, **5**, 1911–1918.

65 C. Ania, B. Cabal, J. Parra and J. Pis, Importance of the hydrophobic character of activated carbons on the removal of naphthalene from the aqueous phase, *Adsorpt. Sci. Technol.*, 2007, **25**, 155–167.

66 J.-H. Choi, J. Jegal and W.-N. Kim, Fabrication and characterization of multi-walled carbon nanotubes/polymer blend membranes, *J. Membr. Sci.*, 2006, **284**, 406–415.

67 C. Raji and T. Anirudha, *Chromium (VI) adsorption by sawdust carbon: Kinetics and equilibrium*, 1997.

68 B.-P. Adrián, I. Didilia and E. Hilda, *Adsorption Processes for Water Treatment and Purification*, Springer, Switzerland, 2017, p. 116.

69 B. Seyhi, P. Drogui, G. Buelna and J. F. Blais, Modeling of sorption of bisphenol A in sludge obtained from a membrane bioreactor process, *Chem. Eng. J.*, 2011, **172**, 61–67.

70 M. Del Bubba, B. Anichini, Z. Bakari, M. C. Bruzzoniti, R. Camisa, C. Caprini, L. Checchini, D. Fibbi, A. El Ghadraoui and F. Liguori, Physicochemical properties and sorption capacities of sawdust-based biochars and commercial activated carbons towards ethoxylated alkylphenols and their phenolic metabolites in effluent wastewater from a textile district, *Sci. Total Environ.*, 2020, **708**, 135217.

71 D. Bonenfant, P. Niquette, M. Mimeault and R. Hausler, Adsorption and recovery of nonylphenol ethoxylate on a crosslinked β-cyclodextrin-carboxymethylcellulose polymer, *Water Sci. Technol.*, 2010, **61**, 2293–2301.

72 A. Ahmad and B. Hameed, Reduction of COD and color of dyeing effluent from a cotton textile mill by adsorption onto bamboo-based activated carbon, *J. Hazard. Mater.*, 2009, **172**, 1538–1543.

73 H. Patel, Characterization and adsorptive treatment of distillery spent wash using bagasse fly ash, *Arabian J. Sci. Eng.*, 2022, **47**, 5521–5531.

74 S. K. Alharbi, M. Shafiquzzaman, H. Haider, S. S. AlSaleem and A. R. Ghumman, Treatment of ablution greywater for recycling by alum coagulation and activated carbon adsorption, *Arabian J. Sci. Eng.*, 2019, **44**, 8389–8399.

75 H. Rubi-Juarez, C. Barrera-Diaz and F. Ureña-Nuñez, Adsorption-assisted electrocoagulation of real car wash wastewater with equilibrium and kinetic studies, *Pollut. Res.*, 2017, **36**, 175–184.

76 A. A. Halim, H. A. Aziz, M. A. M. Johari and K. S. Ariffin, Comparison study of ammonia and COD adsorption on zeolite, activated carbon and composite materials in landfill leachate treatment, *Desalination*, 2010, **262**, 31–35.

 